Brain Stimulation 10 (2017) 19–27

Contents lists available at ScienceDirect

Brain Stimulation

journal homepage: www.brainstimjrnl.com

# Access to Vagal Projections via Cutaneous Electrical Stimulation of the Neck: fMRI Evidence in Healthy Humans

Eleni Frangos *, Barry R. Komisaruk

*Department of Psychology, Rutgers University, 101 Warren St, Newark, NJ 07102, USA*

ARTICLE INFO

*Article history:*
Received 9 July 2016
Received in revised form 13 September 2016
Accepted 16 October 2016
Available online 20 October 2016

*Keywords:*
Vagus nerve
nVNS
Electrical stimulation
Non-invasive
fMRI
NTS

ABSTRACT

*Background:* Stimulation of the vagus nerve via implanted electrodes is currently used to treat refractory epilepsy and depression. Recently, a non-invasive approach to vagal stimulation has demonstrated similar beneficial effects, but it remains unclear whether these effects are mediated via activation of afferent vagal fibers.

*Objective:* The present study was designed to ascertain whether afferent vagal projections can be accessed non-invasively by transcutaneous electrical stimulation of the antero-lateral surface of the neck, which overlies the course of the vagus nerve.

*Methods:* Thirteen healthy subjects underwent 2 fMRI scans in one session. Transcutaneous electrical stimulation was applied for 2 min to the right postero-lateral surface of the neck during scan #1 (control condition, sternocleidomastoid stimulation: "SCM") and to the right antero-lateral surface of the neck during scan #2 (experimental condition, non-invasive vagus nerve stimulation: "nVNS"). Two analyses were conducted using FSL (whole-brain and brainstem; corrected, $p < 0.01$) to determine whether nVNS activated vagal projections in the brainstem and forebrain, compared to baseline and SCM stimulation.

*Results:* Compared to baseline and control (SCM) stimulation, nVNS significantly activated primary vagal projections including: nucleus of the solitary tract (primary central relay of vagal afferents), parabrachial area, primary sensory cortex, and insula. Regions of the basal ganglia and frontal cortex were also significantly activated. Deactivations were found in the hippocampus, visual cortex, and spinal trigeminal nucleus.

*Conclusion:* The present findings provide evidence in humans that cervical vagal afferents can be accessed non-invasively via transcutaneous electrical stimulation of the antero-lateral surface of the neck, which overlies the course of the nerve, suggesting an alternative and feasible method of stimulating vagal afferents.

Published by Elsevier Inc.

## Introduction

Electrical stimulation applied directly to the main trunk of the vagus in the neck via surgically implanted electrodes has been used therapeutically to treat refractory epilepsy and depression, but requires costly invasive surgery and may generate side effects including hoarseness, dyspnea, nausea, pain, and anxiety [1]. Recent developments in *non-invasive* techniques for vagal stimulation, i.e., electrical stimulation of the auricular branch of the vagus nerve ("ABVN"), have demonstrated beneficial effects against epilepsy, depression, and pain [2–5]. Functional brain imaging studies have provided evidence that stimulation of the ABVN accesses central vagal projections [6,7], including the nucleus of the solitary tract ("NTS") [8] which is the first central relay of vagal afferents.

Self-administered transcutaneous electrical stimulation on the antero-lateral surface of the neck superficial to the trajectory of the vagus nerve has been reported recently to abort, and/or reduce the frequency of, acute attacks of cluster headaches even one year after treatment [9]. The non-invasive vagus nerve stimulation (nVNS) device used in that study was a portable, battery-operated device with adjustable intensities and a 2 min electrical stimulus duration. In a proof-of-concept study using the same nVNS approach (i.e., transcutaneous stimulation of the surface of the neck) on a rat model of middle cerebral artery occlusion, Ay et al. [10] reported inhibition of ischemia-induced immune activation, reduction in both tissue damage and functional deficit, and c-Fos labeling

*Abbreviations:* ABVN, auricular branch of the vagus nerve; fMRI, functional magnetic resonance imaging; NTS, nucleus tractus solitarius; nVNS, non-invasive vagus nerve stimulation; SCM, sternocleidomastoid muscle.

* Corresponding author. Fax: 973-353-1171.
*E-mail address:* frangos.eleni@gmail.com (E. Frangos).

1935-861X/Published by Elsevier Inc.
http://dx.doi.org/10.1016/j.brs.2016.10.008

within the NTS, which, they claimed, is indicative of afferent vagus nerve activity.

Despite reports of favorable results using nVNS, it remains unresolved as to whether the effects observed in humans are mediated specifically by nVNS-induced afferent vagus nerve activity. Furthermore, the regional brain responses to nVNS during and after stimulation are unknown. Thus, the present study, using fMRI, was designed to ascertain: (1) whether transcutaneous (non-invasive) electrical stimulation of the neck superficial to the trajectory of the cervical vagus nerve activates vagal afferents, by assessing the activity of the NTS and its projections, and (2) the neural correlates of nVNS during and after stimulation. We mapped brain regions that responded to transcutaneous electrical stimulation of the right antero-lateral surface of the neck (overlying the cervical vagus nerve, "nVNS" condition), compared to stimulation of the control region, overlying the right sternocleidomastoid muscle (postero-lateral surface of the neck, "SCM" condition).

## Materials and methods

The study received approval from the Rutgers University Institutional Review Board; in addition, the "Rutgers University Brain Imaging Center (RUBIC) Common Practices for fMRI" guidelines were strictly followed.

### *Research participants*

Thirteen healthy participants (8 females and 5 males; age range 20–29 years; mean ± SD: 23.1 ± 3.3 years) were recruited for the study by word of mouth and met the inclusion/exclusion criteria: no clinical diagnoses of migraines, epilepsy, depression, or chronic pain; not on medications or claustrophobic; and no MRI-related contraindications. Written informed consent was obtained from each participant. All 13 individuals participated in the two parts of the study: the practice session, and 3–7 days later, the fMRI session consisting of an anatomical scan and two functional scans. In both parts of the study, participants received transcutaneous electrical stimulation at each of two regions of the right surface of the neck: the region of sternocleidomastoid muscle (postero-lateral surface of the neck beneath the earlobe: control condition), and the region of the right cervical vagus nerve (antero-lateral surface of the neck: experimental condition). Placement of the electrodes for the experimental condition was determined by the location of each individual's carotid pulse, as the anatomical location of the cervical vagus nerve courses alongside the carotid artery (Fig. 1). No participants reported discomfort or adverse effects throughout the study, and all received an honorarium for their participation.

### *Stimulation device*

A hand-held battery-operated stimulation device with a pair of non-ferromagnetic stainless steel surface electrodes (1 cm diameter) was used to stimulate the neck. The electrodes were connected to the stimulation unit by an 8-meter-length fMRI-compatible shielded, grounded cable. The non-adjustable parameters of the device were 1-ms duration bursts of 5 sinusoidal wave pulses at 5000 Hz with a repetition rate of 25 Hz, and a continuous train duration of 2 min. The stimulation intensity was adjustable using a dial that ranged from 0 to 5 a.u. (arbitrary units) with a corresponding output ranging from 0 to 48V. In preparing the participant in the fMRI scanner, two separate pairs of electrodes, each pair connected to its own stimulation unit, were applied to the neck, one in the experimental and the other in the control location. Both pairs of electrodes were held in place with a Velcro strap that was adjusted to each person's level of comfort. This enabled the two scans to be performed in succession without necessitating re-adjustment of the electrodes during the scans, thereby minimizing head movement.

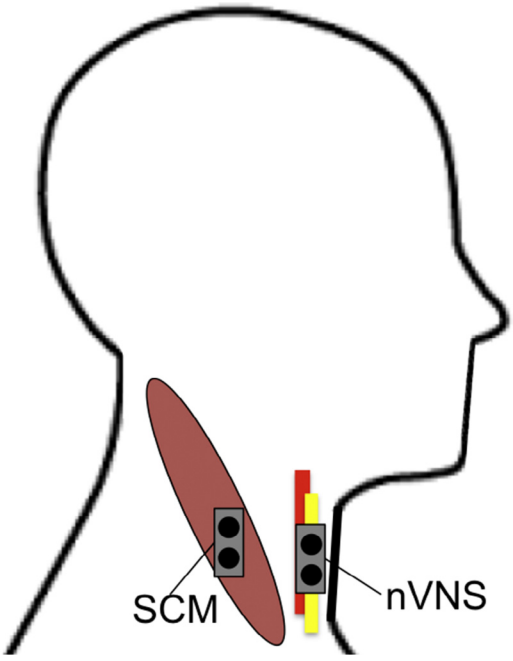


**Figure 1.** Electrode configuration for SCM (control) stimulation over the sternocleidomastoid muscle, and nVNS (experimental) stimulation over the vagus nerve (yellow) as guided by the carotid artery (red). The two pairs of electrodes were held in place with a Velcro strap. (For interpretation of the references to color in this figure legend, the reader is referred to the web version of this article.)

### *Practice session*

The practice session prepared each participant for the fMRI session that took place approximately 3–7 days later. During this session, participants received the actual stimulation as they would in the scanner. Each participant sat upright as the electrodes were applied to the experimental and control locations. Participants were then asked to lie supine on a foam mat in a comfortable position and remain as still as possible during the stimulation procedures. For each condition, they were cued 3 seconds prior to the start of stimulation (blind to the experimental or control condition). Participants were reminded that the stimulation intensity would increase gradually and be set at a comfortable intensity that they would report to us, and should not be tolerated if uncomfortable. At the start of stimulation, the intensity was increased gradually until each participant said, "stop". The stimulation continued at the selected intensity. The duration of stimulation for each condition was 2 min.

In rehearsal for the scanning procedure, each participant watched an accelerated version (approximately 2 min) of the cues that would be shown to them during the actual scanning procedure. They were asked to pay particular attention to the cue requiring them to press a button, as this action would convey to us, the investigators, the signal to stop the gradual increase of the stimulus intensity, and then establish and maintain that intensity during the control and experimental conditions.

The practice session took place in a Rutgers laboratory space outside of the fMRI facility; duration was approximately 20 min.

*fMRI procedure*

The scanning session consisted of an anatomical scan, a field map scan, and two functional scans using a 3T Siemens Trio with a Siemens 12-channel head coil. As in Frangos et al. [8], acquisition parameters were optimized for both whole-brain and lower brainstem regions. Anatomical images were acquired using magnetization prepared rapid gradient echo (MPRAGE) sequences (176 slices in the sagittal plane using 1 mm thick isotropic voxels, TR/TE = 1900 ms/2.52 ms, field-of-view = 256, 256 × 256 matrix, flip angle = 9°; 50% distance factor). Field maps (phase and magnitude) were collected to correct for inhomogeneity in the magnetic field and to increase accuracy of registration during the data analysis. Gradient-echo EPI sequences were acquired of the whole brain including the entire medulla oblongata (33 slices in the axial plane using 3 mm isotropic voxels, TR/TE = 2000 ms/30 ms, interslice gap = 1.5 mm, flip angle = 90°, field-of-view = 192, 64 × 64). The same parameters were used for the field maps with the exception of the flip angle (60°) and TR/TE1/TE2 (400 ms/5.19 ms/7.65 ms). The fMRI-compatible wires and electrodes were passed into the scanner room via a waveguide tube. The stimulation devices remained in the control room, at a distance of approximately 4 meters from the participant in the scanner. While in the scanner room prior to starting the image acquisition protocols, the same two pairs of electrodes were applied to the same experimental and control neck locations used during the practice session. Earplugs were used by each participant and they were instructed to lie down comfortably on the scanner gurney as cushions were placed around the head to restrict movement. A button box was placed under the left hand to be used when cued during the functional scanning procedures. The participants were instructed to remain alert and awake throughout the entire scanning procedure.

*Experimental paradigm*

*Scan #1 – control (SCM) stimulation*

The following data were collected in a 19.5 min scan while subjects viewed a series of travelogue images: rest (2 min), stimulus commencing cue (8 sec), continuous SCM stimulation (2 min; "Press button to stop increase" cue was displayed until button was pressed, then travelogue images continued), and rest (15 min). Synchronization of the stimulation with the scan sequence was performed manually by the same investigator for all participants.

*Scan #2 – experimental (nVNS) stimulation*

Identical sequence, but stimulation was applied via the second pair of electrodes to the surface of the neck overlying the vagus nerve.

The control condition (scan #1) and experimental condition (scan #2) were not counterbalanced, as a carry-over effect was expected from the experimental condition based on findings observed in Frangos et al. [8]. Subjects were blind as to which condition they were going to experience. The interval between the end of scan #1 and beginning of scan #2 was less than 5 min. The average stimulation intensities, as indicated by each participant's perceptual threshold, were 18.7V ± 10.8V for the control condition, and 23.9V ± 12.3V for the experimental condition.

*Data analysis*

All data were preprocessed and statistically analyzed using FMRIB's Software Library ("FSL," Center for Functional Magnetic Resonance Imaging of the Brain, University of Oxford, UK) version 6.00. Lower-level fMRI data processing was carried out using FMRI Expert Analysis Tool (FEAT). The following preprocessing steps were performed at the individual level: removal of skull and non-brain tissue from the anatomical, functional images, and magnitude images, followed by a manual approach to ensure the removal of non-brain tissue around the brainstem; standard motion correction (average motion was <0.5 mm during both stimulation conditions); spatial smoothing using a 5 mm full-width at half-maximum Gaussian kernel; field inhomogeneities were corrected using B0 Unwarping in FEAT; grand-mean intensity normalization; and high pass temporal filtering (Gaussian-weighted least-squares straight line fitting, σ = 600s for scans #1 and #2 [11–15]. For analysis of the brainstem, the above pre-processing analyses were carried out a second time without spatial smoothing to reduce the likelihood of false positives and to enable detection of discrete activity within regions of the brainstem, which are smaller in size than forebrain regions [8,16].

Registration of the functional images to the high-resolution anatomical images was performed using Boundary-Based Registration [17]. High-resolution anatomicals were registered non-linearly to MNI152 standard space using FMRIB's Nonlinear Registration Tool [18,19].

For statistical analyses, the following explanatory variables (EVs) were created at the individual level for the experimental condition and used as regressors to determine the average activity elicited by each condition: whole duration nVNS (2 min), pre-button-press nVNS, post-button-press nVNS, and early (initial 3 min), mid (middle 3 min), and late (last 3 min) post-stimulation. The same process was conducted for the control condition. Higher-level, mixed-effects analyses were carried out to determine mean group effects, followed by contrast analyses to determine differences between nVNS and SCM stimulation. These analyses were carried out once as a whole-brain analysis, and a second time for brainstem analysis using "unsmoothed" data [8,16]. Brainstem regions were localized using the Duvernoy brainstem atlas [20]. Contrast-masking was included to ensure that all contrast results were driven by positive z-statistic voxels of both conditions. All higher-level analyses were corrected for multiple comparisons. The whole-brain and brainstem analyses were processed with a cluster-significance threshold of p = 0.01 and p = 0.001, respectively. The range of z-scores for each analysis is indicated on each figure (the lower interval indicates the cluster-forming threshold for that particular analysis).

## Results

The findings are summarized in Table 1.

*Active stimulation period*

*Whole-brain analyses*

*nVNS compared to baseline.* Classical vagal projections were activated in response to the 2 min nVNS stimulation. By comparison with baseline, bilateral activation was observed in: the "visceral region" of the primary sensory cortex (S1), the operculum, anterior-, mid- and posterior insula, dorsolateral prefrontal cortex, anterior cingulate cortex, supramarginal gyrus, thalamus, caudate, and putamen. Contralateral (left) activation was observed in the lateral occipital and middle temporal cortices and cerebellum. Ipsilateral activation was observed in the superior frontal and orbitofrontal cortices, and in the supplementary motor area. Extensive deactivation was found bilaterally in visual areas, and in the right hippocampus and parahippocampus (Fig. 2).

*SCM compared to baseline.* The control stimulation condition (sternocleidomastoid muscle) activated the following forebrain regions: bilateral posterior insula, operculum, and neck/shoulder region of S1. Contralateral activation was observed in the primary motor cortex. Deactivation was found in the visual cortex.

**Table 1**
Significant findings with coordinates of max z-score.

| Active stimulation period | | | | |
|---|---|---|---|---|
| Whole-brain | | | | |
| nVNS > BL | z-score | x | y | z |
| Activations | | | | |
| Left | | | | |
| Anterior cingulate | 3.87 | –2 | 22 | 34 |
| Caudate | 3.16 | –12 | –2 | 16 |
| Cerebellum | 3.89 | –32 | –72 | –32 |
| Dorsal lateral prefrontal cortex | 4.16 | –30 | 32 | 40 |
| Insula | 3.39 | –38 | 2 | 4 |
| Lateral occipital cortex/mid-temporal gyrus | 3.86 | –62 | –62 | 6 |
| Operculum | 3.35 | –58 | –18 | 16 |
| Putamen | 3.15 | –22 | 10 | 8 |
| Primary sensory cortex | 4.14 | –60 | –20 | 30 |
| Supramarginal gyrus | 4.16 | –62 | –38 | 36 |
| Thalamus | 3.83 | –10 | –16 | 10 |
| Right | | | | |
| Orbitofrontal cortex | 3.33 | 40 | 30 | –2 |
| Supplementary motor area | 3.13 | 4 | 4 | 66 |
| Anterior cingulate | 4.13 | 10 | 34 | 12 |
| Caudate | 3.93 | 16 | 24 | 6 |
| Dorsal lateral prefrontal cortex | 4.01 | 54 | 20 | 36 |
| Insula | 4.11 | 38 | 20 | 0 |
| Operculum | 3.87 | 36 | 2 | 16 |
| Putamen | 3.11 | 24 | 12 | –4 |
| Primary sensory cortex | 3.21 | 58 | –14 | 30 |
| Superior frontal cortex | 4.68 | 20 | 10 | 64 |
| Supramarginal gyrus | 4.30 | 58 | –44 | 52 |
| Thalamus | 2.83 | 18 | –16 | 12 |
| Deactivations | | | | |
| Left | | | | |
| Lateral occipital cortex | 3.31 | –28 | –88 | 18 |
| Temporal occipital fusiform cortex | 3.66 | –28 | –48 | –8 |
| Right | | | | |
| Hippocampus | 3.14 | 32 | –16 | –16 |
| Lateral occipital cortex | 3.67 | 32 | –78 | 22 |
| Parahippocampus | 3.04 | 30 | –28 | –20 |
| Temporal occipital fusiform cortex | 4.28 | 26 | –46 | –12 |
| SCM > BL | z-score | x | y | z |
| Activations | | | | |
| Left | | | | |
| Operculum | 3.87 | –52 | –36 | 20 |
| Posterior insula | 4.24 | –36 | –18 | 16 |
| Premotor cortex | 3.98 | –12 | –12 | 68 |
| Primary sensory cortex | 3.96 | –20 | –44 | 62 |
| Right | | | | |
| Insula | 3.74 | 44 | –6 | 0 |
| Operculum | 3.80 | 40 | –20 | 20 |
| Primary sensory cortex | 5.61 | 26 | –38 | 68 |
| Deactivations | | | | |
| Lateral occipital cortex | 3.28 | 38 | –84 | –8 |
| nVNS > SCM | z-score | x | y | z |
| Activations | | | | |
| Left | | | | |
| Dorsal lateral prefrontal cortex | 4.01 | –30 | 32 | 40 |
| Anterior cingulate | 3.16 | –2 | 16 | 34 |
| Caudate | 3.04 | –12 | –2 | 16 |
| Cerebellum | 3.90 | –32 | –70 | –28 |
| Lateral occipital cortex | 3.75 | –50 | –74 | –12 |
| Paracingulate | 3.56 | –2 | 42 | 30 |
| Primary sensory cortex (visceral) | 3.13 | –60 | –20 | 30 |
| Supramarginal gyrus | 3.88 | –52 | –42 | 56 |
| Thalamus | 3.70 | –10 | –16 | 10 |
| Right | | | | |
| Dorsal lateral prefrontal cortex | 3.49 | 52 | 16 | 42 |
| Anterior cingulate | 4.04 | 10 | 36 | 12 |
| Anterior insula | 3.15 | 38 | 22 | 0 |
| Caudate | 3.72 | 16 | 20 | 8 |
| Paracingulate | 4.20 | 2 | 38 | 36 |
| Putamen | 2.70 | 24 | 12 | –4 |
| Superior frontal gyrus | 4.45 | 22 | 12 | 68 |
| Thalamus | 2.97 | 18 | –16 | 12 |
| Brainstem (unsmoothed) | | | | |
| nVNS > SCM | z-score | x | y | z |
| Activations | | | | |
| Left | | | | |
| Parabrachial area | 1.21 | –4 | –40 | –22 |
| Ventral tegmental area | 1.21 | –2 | –22 | –14 |
| Nucleus cuneiformis | 1.32 | –4 | –26 | –14 |
| Brachium conjunctivum | 1.46 | –2 | –24 | –14 |
| Right | | | | |
| Medial longitudinal fasciculus | 1.06 | 0 | –42 | –60 |
| Nucleus of the solitary tract (NTS) | 1.14 | 2 | –46 | –58 |
| NTS/dorsal motor nucleus of vagus | 1.32 | –4 | –44 | –52 |
| Parabrachial area | 1.39 | 6 | –40 | –22 |
| Substantia nigra | 1.58 | 16 | –16 | –12 |
| Vestibular nucleus | 1.67 | 4 | –44 | –46 |
| Nucleus cuneiformis | 1.09 | 8 | –28 | –18 |
| Deactivations | | | | |
| Left | | | | |
| Nucleus of the solitary tract | 1.32 | –2 | –46 | –60 |
| Corticospinal tract | 1.91 | –2 | –34 | –60 |
| Pontine nuclei | 1.93 | –6 | –26 | –32 |
| Right | | | | |
| Spinal trigeminal nucleus caudalis | 1.26 | 6 | –44 | –60 |
| Post-nVNS period | | | | |
| Whole-brain | | | | |
| Early post-nVNS | z-score | x | y | z |
| Deactivations | | | | |
| Left | | | | |
| Medial frontal cortex | 3.04 | –4 | 32 | –24 |
| Medial temporal gyrus | 4.13 | –54 | –20 | –8 |
| Paracingulate | 3.63 | –2 | 42 | 28 |
| Right | | | | |
| Medial frontal cortex | 3.71 | 2 | 36 | –24 |
| Paracingulate | 2.94 | 2 | 42 | 30 |
| Mid-post-nVNS | z-score | x | y | z |
| Activations | | | | |
| Left | | | | |
| Anterior cingulate | 2.55 | –2 | 38 | 2 |
| Hypothalamus | 3.15 | –4 | 0 | –6 |
| Parahippocampus | 2.76 | –32 | –34 | –14 |
| Precuneus | 3.50 | –8 | –52 | 10 |
| Thalamus | 2.84 | –20 | –30 | 6 |
| Right | | | | |
| Amygdala | 3.01 | 24 | –4 | –16 |
| Anterior cingulate | 2.67 | 6 | 22 | 20 |
| Anterior insula | 3.52 | 32 | 18 | –4 |
| Hippocampus | 2.42 | 30 | –10 | –20 |
| Precuneus | 3.13 | 16 | –52 | 16 |
| Thalamus | 2.75 | 8 | –8 | 0 |
| Late post-nVNS | z-score | x | y | z |
| Activations | | | | |
| Left | | | | |
| Cerebellum | 3.62 | –32 | –52 | –50 |
| Precentral gyrus | 3.15 | –32 | –16 | 52 |
| Precuneus | 3.50 | –6 | –54 | 36 |
| Putamen | 3.14 | –22 | 18 | –2 |
| Superior frontal gyrus | 3.52 | –4 | 36 | 44 |
| Thalamus | 3.19 | –4 | –12 | 8 |
| Right | | | | |
| Caudate | 2.67 | 14 | 8 | 12 |
| Precentral gyrus | 3.50 | 12 | –28 | 62 |
| Precuneus | 3.38 | 8 | –70 | 50 |
| Superior frontal gyrus | 3.56 | 16 | 4 | 62 |
| Thalamus | 2.96 | 6 | –24 | 8 |
| Brainstem (unsmoothed) | | | | |
| Early post-nVNS | z-score | x | y | z |
| Right | | | | |
| Substantia nigra | 2.25 | 8 | –18 | –18 |
| Midline | | | | |
| Dorsal raphe nucleus | 2.09 | 0 | –30 | –22 |

(*continued on next page*)

**Table 1** (*continued*)

| Mid-post-nVNS | z-score | x | y | z |
|---|---|---|---|---|
| Left | | | | |
| Dorsal raphe nuclei | 1.43 | –2 | –28 | –18 |
| Right | | | | |
| Nucleus cuneiformis | 2.35 | 8 | –28 | –16 |
| Midline | | | | |
| Periaqueductal gray | 1.41 | 0 | –32 | –18 |
| Ventral tegmental area | 1.76 | 0 | –24 | –18 |
| **Late post-nVNS** | **z-score** | **x** | **y** | **z** |
| Left | | | | |
| Dorsal raphe nuclei | 1.68 | –2 | –28 | –18 |
| Right | | | | |
| Nucleus cuneiformis | 2.61 | 10 | –26 | –14 |
| Substantia nigra | 1.98 | 8 | –20 | –16 |
| Midline | | | | |
| Periaqueductal gray | 1.64 | 0 | –32 | –18 |
| Ventral tegmental area | 1.84 | 0 | –24 | –18 |

Note: Whole-brain analyses – corrected, $p < 0.01$; brainstem analyses – unsmoothed; corrected, $p < 0.001$.

*nVNS > SCM.* By comparison of nVNS with control, muscle stimulation (Fig. 3), bilateral activation was observed in: dorsolateral prefrontal, paracingulate and anterior cingulate cortices, caudate, and thalamus. Contralateral activation was observed in the "visceral region" of S1, supramarginal and lateral occipital cortices, and cerebellum. Ipsilateral activation was observed in the superior frontal and premotor cortices, anterior insula, and putamen. No regions were activated significantly more by SCM than by nVNS (i.e., in the SCM > nVNS comparison).

*Lower brainstem analyses*

To avoid activation of brainstem nuclei responsive to movement and sensation associated with the participants' button press, we analyzed the "post-button press" period of the 2 min nVNS and SCM stimulation conditions. Within the lower brainstem, we found significantly greater activation in response to nVNS than to SCM (nVNS > SCM) in the following regions: ipsilateral (right) NTS, region of contralateral NTS/dorsal motor nucleus of the vagus, medial longitudinal fasciculus, vestibular nuclei, bilateral parabrachial area, and nuclei cuneiformis, and contralateral (left) brachium conjunctivum; scattered activation was observed in the substantia nigra and ventral tegmental area (Figs. 4 and 5). Significant deactivations in response to nVNS were observed in the region of the contralateral (left) NTS, the cortical spinal tract, and pontine nuclei, and in the ipsilateral (right) spinal trigeminal nucleus caudalis (Fig. 5).

The lower brainstem analysis indicated that the NTS, which is the first central relay of vagal afferents, was significantly activated during nVNS by comparison with SCM stimulation.

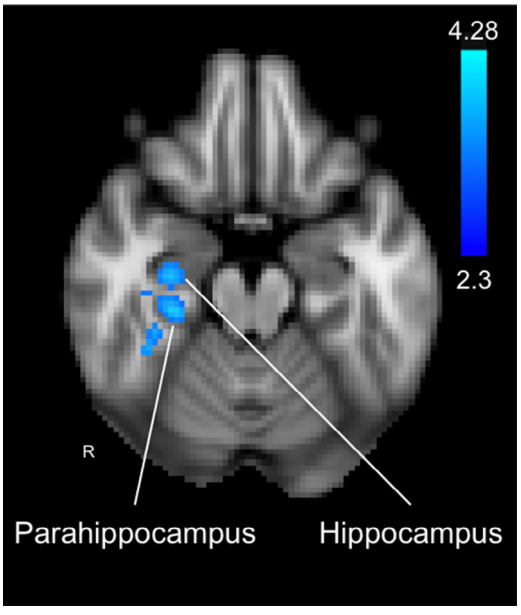


**Figure 2.** During the 2 min nVNS period, deactivation (baseline > nVNS) was observed in the hippocampus and parahippocampus (z = 26). R: right.

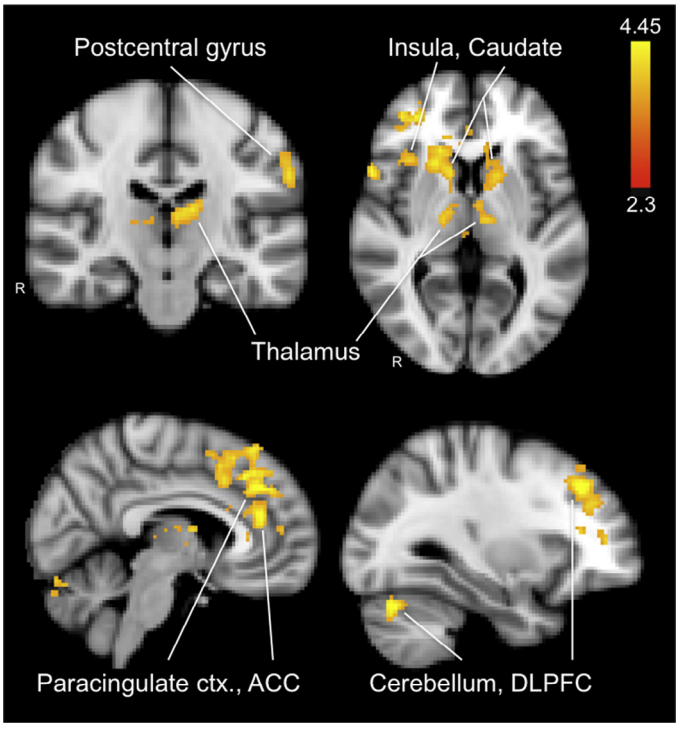


**Figure 3.** The labeled brain regions showed significantly greater activity during nVNS stimulation (right antero-lateral neck region overlying the vagus nerve) than during SCM, control, stimulation (right postero-lateral neck region). Slice coordinates, clockwise from top left: y = 53, z = 38, x = 60, x = 42. Abbreviations: ACC: anterior cingulate cortex; DLPFC: dorsolateral prefrontal cortex. R: right.

*Post-nVNS period*

*Whole-brain analyses*

Based on other vagus stimulation paradigms in which behavioral effects persisted beyond the stimulation period, we analyzed the activity in the 15 min post-stimulation period by dividing it into 3 phases – early (minutes 1–3), middle (minutes 7–9), and late (minutes 13–15).

In the forebrain, during the initial post-nVNS period, we found no significant regional activation; however, there was deactivation of the medial frontal and paracingulate cortices (bilateral), and medial temporal gyrus (contralateral). Similarly, in the late post-stimulation period, there was no significant regional activation, but extensive deactivation of regions including the bilateral thalamus, superior frontal gyrus, precentral gyrus, and precuneus, contralateral putamen and cerebellum, and ipsilateral caudate.

By striking contrast, the following brain regions became activated during the mid-post-stimulation period (compared to baseline): ipsilateral hippocampus, amygdala, and anterior insula, contralateral parahippocampal gyrus and hypothalamus, bilateral thalamus, precuneus, anterior cingulate, and prefrontal cortex (Fig. 6).

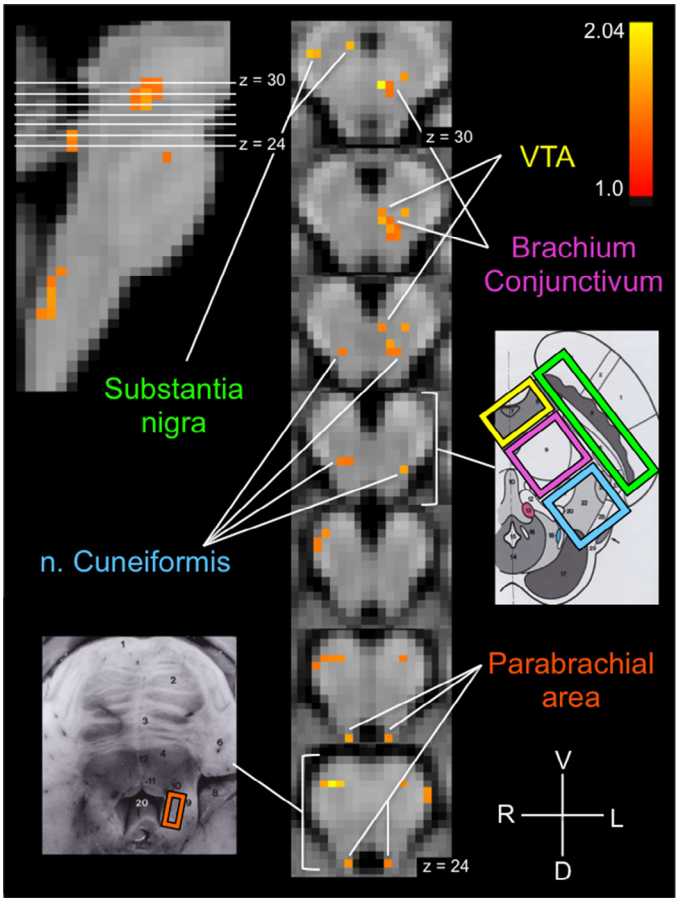


**Figure 4.** The labeled upper brainstem regions showed significantly greater activity during the nVNS condition compared to the SCM, control, stimulation condition. These and subsequent schematic diagrams are modified from the Naidich et al. [20] atlas. Abbreviations: n.: nucleus; VTA: ventral tegmental area; V: ventral; D: dorsal; R: right; L: left.

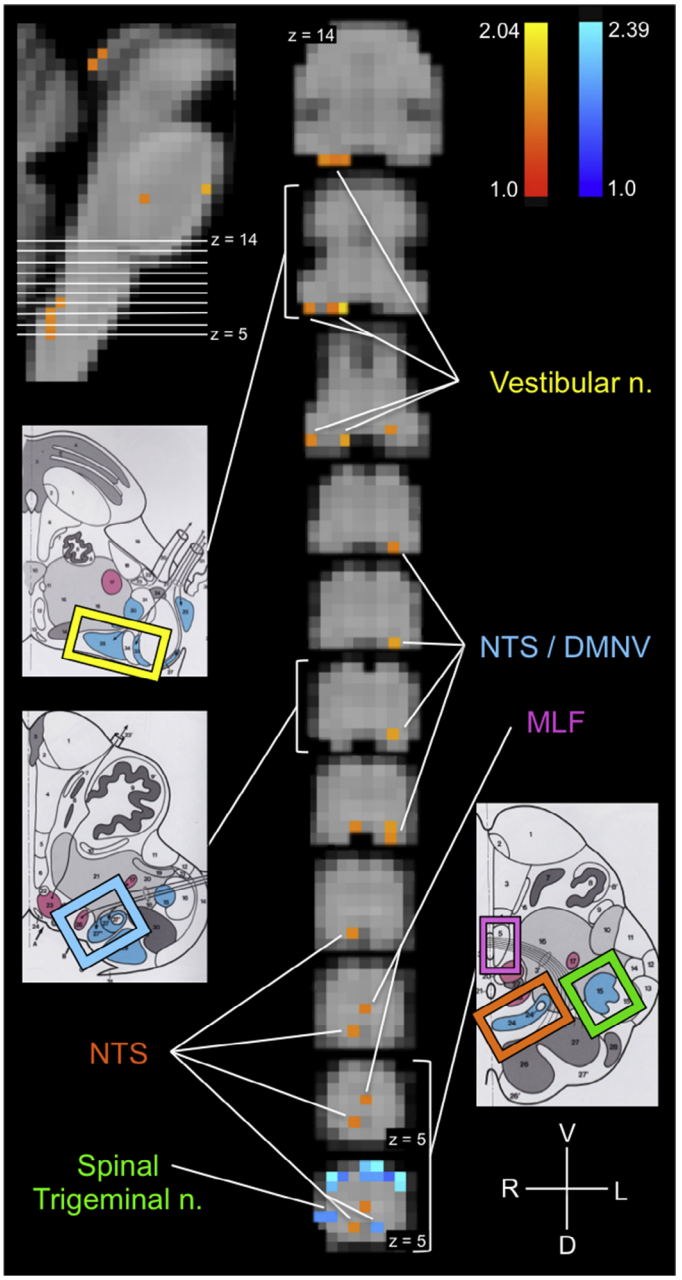


**Figure 5.** The labeled lower brainstem regions showed significantly greater activity during the nVNS condition compared to the SCM, control, stimulation condition. Deactivations observed during nVNS are shown on the last horizontal slice (z = 5) alongside the activations observed in the above contrast analysis. Abbreviations: DMNV: dorsal motor nucleus of the vagus; MLF: medial longitudinal fasciculus; n.: nucleus; NTS: nucleus of the solitary tract; V: ventral; D: dorsal; R: right; L: left.

*Lower brainstem analyses*

During the early post-nVNS period, activations were observed in the substantia nigra and dorsal raphe nuclei. The ventral tegmental area (VTA), periaqueductal gray (PAG), and nucleus cuneiformis became activated during the mid post-nVNS period and the dorsal raphe remained activated. Activation in all these regions persisted throughout the late post-nVNS period, including activation in the substantia nigra (Fig. 6).

There was less deactivation in the lower brainstem during the mid-post nVNS phase than during the early or late post-nVNS phases. This is consistent with the greater activation in forebrain during this mid-phase, and the greater deactivation of forebrain during the post-nVNS early and late phases.

## Discussion

The present study provides fMRI evidence in 13 healthy adults that mild electrical stimulation of the antero-lateral surface of the neck, in the region overlying the course of the vagus nerve, compared to stimulation of the postero-lateral surface of the neck, activated classical vagal projections, e.g., NTS (ipsilateral), parabrachial area, insula, lateral S1, thalamus, and caudate, and deactivated the hippocampus, contralateral NTS, and ipsilateral spinal trigeminal nucleus. In addition to these classical vagal projections, we observed activation of regions in the lower brainstem involved in proprioception and pain modulation. The post-nVNS period was characterized by a dramatic biphasic pattern of initial deactivation, followed by a mid-phase of significant activation that included regions different from those during stimulation, followed by a secondary overall deactivation in cortical, subcortical, and cerebellar regions. Post-nVNS activations in the brainstem were found within regions different from those during stimulation, specifically in the substantia nigra, VTA, dorsal raphe nuclei, and periaqueductal gray.

While not directly comparable, nevertheless, the observed regional brain activity in this study on healthy participants is analogous to that reported for invasive stimulation of the left cervical vagus nerve in patients with epilepsy and depression; e.g., insula, thala-

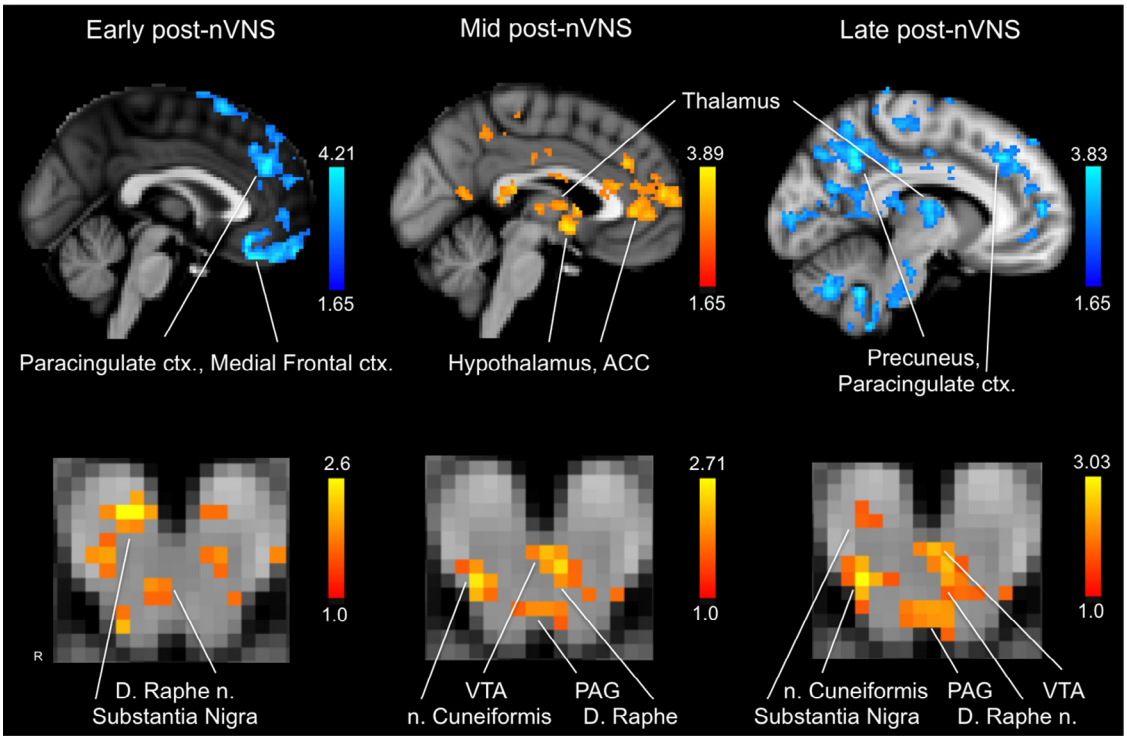


**Figure 6.** After the cessation of the nVNS stimulation, brain activity changed in a biphasic pattern. We divided the 15 min post-stimulation period into three 3-min phases and compared each phase to baseline: "Early" (the first 3 min upon cessation of the stimulation), "Mid" (min 7–9), and "Late" (min 13–15). Upper row: During the Early phase, there was significant deactivation (activity significantly lower than during the baseline, pre-nVNS period) in the labeled regions. By striking contrast, there was a "rebound" activation of the regions shown during the Mid phase. Deactivation returned in widespread brain regions during the Late phase. Slice coordinates from left to right: x = 45, x = 46, x = 49. Lower row: In the lower brainstem (z = 27), activation persisted after cessation of nVNS in the labeled regions. Abbreviations: PAG: periaqueductal gray; VTA: ventral tegmental area; D. Raphe n.: dorsal raphe nucleus. R: right.

mus, hypothalamus, postcentral gyrus, middle temporal gyrus, cerebellum, and superior, middle, and orbitofrontal gyri [21–33]. Similar regional activity was reported with non-invasive stimulation of the external ear in regions innervated by the auricular branch of the vagus nerve [6–8,34].

A unique pattern of activation in the brainstem was observed in response to nVNS in the present study that was not previously reported by others who investigated the neural correlates of afferent vagal stimulation in humans. That is, in the present study, nVNS activated both the vagal afferent pathway and brainstem regions involved in proprioception and baroreceptor activation, as would occur in the orthostatic reflex. In this reflex, changes in blood pressure are detected by baroreceptors, which project to the NTS and parabrachial nuclei, in response to changes in posture and head position, which are detected by the vestibular system. The latter involves vestibular and parabrachial nuclei, the medial longitudinal fasciculus, brachium conjunctivum, and cerebellum, each of which was activated by nVNS in the present study. A classical effect of direct stimulation of the baroreceptors is profound vasodilation [35]. There is evidence that cluster headaches are associated with increased hypertension during an attack [36,37]. Thus, it is possible that one of the mechanisms by which cluster headache frequency and attacks were reduced and aborted, respectively, with nVNS in the study by Nesbitt et al. [9] was by inducing *hypo*-tension through suprathreshold activation of the carotid baroreceptors.

In 2002, Goadsby [38] implicated the hypothalamus in cluster headache on the basis of structural and neuroendocrine changes observed in chronic sufferers.

A case report of the long-term effects of deep brain stimulation (DBS) of the hypothalamus for intractable cluster headache indicated that the treatment was successful [39], although a subsequent study did not replicate this finding [40]. Nesbitt et al. [9] reported an 11 min delayed onset of cluster headache attenuation in response to nVNS using the same parameters as the present study. Consistent with the Nesbitt et al. [9] report, we found a 10 min lag in the activation of the hypothalamus in response to nVNS. Thus, a possible mechanism by which nVNS attenuates cluster headache is via its ability to modulate hypothalamic activity.

Analgesic effects other than headache attenuation may occur in response to nVNS-evoked activation of the dorsolateral prefrontal cortex, as this region is implicated in antinociceptive responses against experimental and chronic pain [41,42]. The post-nVNS activation observed in the raphe nuclei and PAG in the present study is consistent with the effects of non-invasive vagal stimulation via the external ear [8] and may activate the descending pain-inhibitory pathways in the spinal cord [43,44]. The activation of nucleus cuneiformis observed during and after nVNS is of particular interest, as this nucleus has been shown in rats to respond to vagal stimulation [45] and to activate the descending pain-modulatory system [46]. Furthermore, deactivation of the spinal trigeminal nucleus in response to nVNS suggests a role for nVNS in countering trigeminal nociception. In 2003, Bohotin et al. [47] showed that invasive VNS inhibited formalin-induced Fos-expression within the spinal trigeminal nucleus in rats. Recently, Oshinsky et al. [48] reported in rats, that administration of glyceryl trinitrate induced periorbital trigeminal allodynia and significantly elevated the nociception-inducing excitatory amino acid, glutamate, in the extracellular space of the spinal trigeminal nucleus caudalis. After 2min of nVNS, periorbital sensitivity was reduced and elevated extracellular levels of glutamate were significantly reversed.

The deactivation of the hippocampus observed in the present study suggests a possible role for nVNS in attenuating seizure

activity in patients with intractable epilepsy. These findings corroborate those of other studies reporting on afferent vagal stimulation in epilepsy patients [49] and healthy participants [7,8].

## Limitations

The control stimulation condition was mild transcutaneous stimulation of the postero-lateral neck region, overlying the sternocleidomastoid muscle (SCM). While NTS activation was not observed in response to SCM stimulation, the data analysis indicated that this "control" stimulus activated a distribution of brain regions that overlapped, to a limited extent, those activated much more extensively by stimulation of the (experimental, nVNS) antero-lateral neck region, which overlies the vagal trunk. Based on these findings, we conclude that SCM stimulation is not an optimal control for antero-lateral "vagal" neck stimulation because it seems to activate the vagal trunk to some extent, possibly by spread of current. Consequently, a more remote stimulation site is advisable as a control condition. Nevertheless, it is possible that stimulation of the SCM activates brain regions similar to those activated by vagal afferents, independent of spread of current, as brain regions typically respond to more than one type of stimulus. However, as there was an indication of possible vagal activation in response to the muscle stimulation – as indicated by bilateral operculum and posterior insula activation – caution in interpretation of nVNS > SCM is advisable.

## Conclusion

The present findings provide evidence in humans that cervical vagal afferents can be accessed non-invasively via transcutaneous electrical stimulation of the antero-lateral surface of the neck (nVNS), which overlies the course of the vagus nerve. The regional brain activation elicited by nVNS is analogous to that elicited by invasive vagus nerve stimulation and other forms of non-invasive vagus stimulation, specifically that applied to the external ear in the sensory field of the auricular branch of the vagus nerve. While more research is needed to evaluate the therapeutic efficacy of nVNS, ease of use and application of nVNS render it feasible to test its effectiveness against disorders that are responsive to afferent vagal stimulation.

## Acknowledgements

This study was supported by electroCore, LLC and the Rutgers Institute for Data Science, Learning, and Applications (IDSLA).

## References

[1] Cristancho P, Cristancho MA, Baltuch GH, Thase ME, O'Reardon JP. Effectiveness and safety of vagus nerve stimulation for severe treatment-resistant major depression in clinical practice after FDA approval: outcomes at 1 year. J Clin Psychiatry 2011;72:1376–82.
[2] Busch V, Zeman F, Heckel A, Menne F, Ellrich J, Eichhammer P. The effect of transcutaneous vagus nerve stimulation on pain perception – an experimental study. Brain Stimul 2013;6:202–9.
[3] Hein E, Nowak M, Kiess O, Biermann T, Bayerlein K, Kornhuber J, et al. Auricular transcutaneous electrical nerve stimulation in depressed patients: a randomized controlled pilot study. J Neural Transm 2013;120:821–7.
[4] Rong PJ, Zhao JJ, Li YQ, Litscher D, Li SY, Gaischek I, et al. Auricular acupuncture and biomedical research–a promising Sino-Austrian research cooperation. Chin J Integr Med 2015;21(12):887–94.
[5] Stefan H, Kreiselmeyer G, Kerling F, Kurzbuch K, Rauch C, Heers M, et al. Transcutaneous vagus nerve stimulation (t-VNS) in pharmacoresistant epilepsies: a proof of concept trial. Epilepsia 2012;53:e115–18.
[6] Dietrich S, Smith J, Scherzinger C, Hofmann-Preiss K, Feitag T, Eisenkolb A, et al. A novel transcutaneous vagus nerve stimulation leads to brainstem and cerebral activations measured by functional MRI. Biomed Tech (Berl) 2008;53:104–11.
[7] Kraus T, Hösl K, Kiess O, Schanze A, Kornhuber J, Forster C. BOLD fMRI deactivation of limbic and temporal brain structures and mood enhancing effect by transcutaneous vagus nerve stimulation. J Neural Transm 2007;114:1485–93.
[8] Frangos E, Ellrich J, Komisaruk BR. Non-invasive access to the vagus nerve central projections via electrical stimulation of the external ear: fMRI evidence in humans. Brain Stimul 2015;8(3):624–36.
[9] Nesbitt A, Marin JCA, Tompkins E, Ruttledge M, Goadsby P. Initial use of a novel noninvasive vagus nerve stimulator for cluster headache treatment. Neurology 2015;84(12):1249–53.
[10] Ay I, Nasser R, Simon B, Ay H. Transcutaneous cervical vagus nerve stimulation ameliorates acute ischemic injury in rats. Brain Stimul 2015;9(2):166–73.
[11] Jenkinson M, Bannister P, Brady M, Smith S. Improved optimisation for the robust and accurate linear registration and motion correction of brain images. Neuroimage 2002;17:825–41.
[12] Jenkinson M, Smith SM. A global optimisation method for robust affine registration of brain images. Med Image Anal 2001;5:143–56.
[13] Jenkinson M. A fast, automated, n-dimensional phase unwrapping algorithm. Magn Reson Med 2003;49:193–7.
[14] Jenkinson M. Improving the registration of B0-distorted EPI images using calculated cost function weights. In: Tenth international conference on functional mapping of the human brain; 2004.
[15] Woolrich MW, Ripley BD, Brady JM, Smith SM. Temporal autocorrelation in univariate linear modelling of FMRI data. Neuroimage 2001;14:1370–86.
[16] Poldrack RA, Mumford JA, Nichols TE. Handbook of functional MRI data analysis. New York: Cambridge University Press; 2011.
[17] Greve DN, Fischl B. Accurate and robust brain image alignment using boundary-based registration. Neuroimage 2009;48:63–72.
[18] Andersson JLR, Jenkinson M, Smith SM. Non-linear optimisation. FMRIB technical report TR07JA1; 2007a.
[19] Andersson JLR, Jenkinson M, Smith SM. Non-linear registration, aka spatial normalisation. FMRIB technical report TR07JA2; 2007b.
[20] Naidich TP, Duvernoy HM, Delman BN, Sorensen AG, Kollias SS, Haacke EM. Duvernoy's atlas of the human brain stem and cerebellum. Vienna: Springer-Verlag/Wien; 2009.
[21] Bohning DE, Lomarev MP, Denslow S, Nahas Z, Shastri A, George MS. Feasibility of vagus nerve stimulation-synchronized blood oxygenation level- dependent functional MRI. Invest Radiol 2001;36(8):470–9.
[22] Conway CR, Sheline YI, Chibnall JT, Bucholz RD, Price JL, Gangwani S, et al. Brain blood-flow change with acute vagus nerve stimulation in treatment-refractory major depressive disorder. Brain Stimul 2012;5(2):163–71.
[23] Conway CR, Chibnall JT, Gebara MA, Price JL, Snyder AZ, Mintun MA, et al. Association of cerebral metabolic activity changes with vagus nerve stimulation antidepressant response in treatment-resistant depression. Brain Stimul 2013;6(5):788–97.
[24] Critchley HD, Lewis PA, Orth M, Josephs O, Deichmann R, Trimble MR, et al. Vagus nerve stimulation for treatment-resistant depression: behavioral and neural effects on encoding negative material. Psychosom Med 2007;69(1):17–22.
[25] Ko D, Heck C, Grafton S, Apuzzo ML, Couldwell WT, Chen T, et al. Vagus nerve stimulation activates central nervous system structures in epileptic patients during PET H2(15)O blood flow imaging. Neurosurgery 1996;39(2):426–30.
[26] Kosel M, Brockmann H, Frick C, Zobel A, Schlaepfer TE. Chronic vagus nerve stimulation for treatment-resistant depression increases regional cerebral blood flow in the dorsolateral prefrontal cortex. Psychiatry Res 2011;191(3):153–9.
[27] Liu WC, Mosier K, Kalnin AJ, Marks D. BOLD fMRI activation induced by vagus nerve stimulation in seizure patients. J Neurol Neurosurg Psychiatry 2003;74:811–13.
[28] Lomarev M, Denslow S, Nahas Z, Chae JH, George MS, Bohning DE. Vagus nerve stimulation (VNS) synchronized BOLD fMRI suggests that VNS in depressed adults has frequency/dose dependent effects. J Psychiatr Res 2002;36(4):219–27.
[29] Nahas Z, Teneback C, Chae JH, Mu Q, Molnar C, Kozel FA, et al. Serial vagus nerve stimulation functional MRI in treatment-resistant depression. Neuropsychopharmacology 2007;32(8):1649–60.
[30] Narayanan JT, Watts R, Haddad N, Labar DR, Li PM, Filippi CG. Cerebral activation during vagus nerve stimulation: a functional MR study. Epilepsia 2002;43(12):1509–14.
[31] Pardo JV, Sheikh SA, Schwindt GC, Lee JT, Kuskowski MA, Surerus C, et al. Chronic vagus nerve stimulation for treatment-resistant depression decreases resting ventromedial prefrontal glucose metabolism. Neuroimage 2008;42(2):879–89.
[32] Sucholeiki R, Alsaadi TM, Morris GL 3rd, Ulmer JL, Biswal B, Mueller WM. fMRI in patients implanted with a vagal nerve stimulator. Seizure 2002;11(3):157–62.
[33] Vonck K, De Herdt V, Bosman T, Dedeurwaerdere S, Van Laere K, Boon P. Thalamic and limbic involvement in the mechanism of action of vagus nerve stimulation, a SPECT study. Seizure 2008;17(8):699–706.
[34] Kraus T, Kiess O, Hösl K, Terekhin P, Kornhuber J, Forster C. CNS BOLD fMRI effects of sham-controlled transcutaneous electrical nerve stimulation in the left outer auditory canal – a pilot study. Brain Stimul 2013;6(5):798–804.
[35] Vatner SF, Franklin D, Van Citters RL, Braunwald E. Effects of carotid sinus nerve stimulation on blood-flow distribution in conscious dogs at rest and during exercise. Circ Res 1970;27(4):495–503.
[36] Nordin M, Fagius J, Waldenlind E. Sympathetic vasoconstrictor outflow to extremity muscles in cluster headache. Recordings during spontaneous and nitroglycerin-induced attacks. Headache 1997;37(6):358–67.
[37] Russell D, von der Lippe A. Cluster headache: heart rate and blood pressure changes during spontaneous attacks. Cephalalgia 1982;2(2):61–70.
[38] Goadsby PJ. Pathophysiology of cluster headache: a trigeminal autonomic cephalgia. Lancet Neurol 2002;1(4):251–7.

[39] Leone M, Franzini A, Broggi G, May A, Bussone G. Long-term follow-up of bilateral hypothalamic stimulation for intractable cluster headache. Brain 2004;127:2259–64.
[40] Pinsker MO, Bartsch T, Falk D, Volkmann J, Herzog J, Steigerwald F, et al. Failure of deep brain stimulation of the posterior inferior hypothalamus in chronic cluster headache-report of two cases and review of the literature. Zentralbl Neurochir 2008;69(2):76–9.
[41] Brighina F, De Tommaso M, Giglia F, Scalia S, Cosentino G, Puma A, et al. Modulation of pain perception by transcranial magnetic stimulation of left prefrontal cortex. J Headache Pain 2011;12:185–91.
[42] Seminowicz DA, Wideman TH, Naso L, Hatami-Khoroushahi Z, Fallatah S, Ware MA, et al. Effective treatment of chronic low back pain in humans reverses abnormal brain anatomy and function. J Neurosci 2011;31(20):7540–50.
[43] Basbaum AI, Fields HL. Endogenous pain control mechanisms: review and hypothesis. Ann Neurol 1978;4:451–62.
[44] Millan MJ. Descending control of pain. Prog Neurobiol 2002;66:355–474.
[45] Mönnikes H, Rüter J, König M, Grote C, Kobelt P, Klapp BF, et al. Differential induction of c-fos expression in brain nuclei by noxious and non-noxious colonic distension: role of afferent C-fibers and 5-HT3 receptors. Brain Res 2003;966:253–64.
[46] Zemlan FP, Behbehani MM. Nucleus cuneiformis and pain modulation: anatomy and behavioral pharmacology. Brain Res 1988;453:89–102.
[47] Bohotin C, Scholsem M, Multon S, Martin D, Bohotin V, Schoenen J. Vagus nerve stimulation in awake rats reduces formalin-induced nociceptive behavior and fos-immunoreactivity in trigeminal nucleus caudalis. Pain 2003;101:3–12.
[48] Oshinsky ML, Murphy AL, Hekierski H Jr, Cooper M, Simon BJ. Noninvasive vagus nerve stimulation as treatment for trigeminal allodynia. Pain 2014;155(5):1037–42.
[49] Henry TR, Bakay RA, Votaw JR, Pennell PB, Epstein CM, Faber TL, et al. Brain blood flow alterations induced by therapeutic vagus nerve stimulation in partial epilepsy: I. Acute effects at high and low levels of stimulation. Epilepsia 1998;39:983–90.